Geological Quarterly, 2025, 69, 27
DOI: https://doi.org/10.7306/gq.1800

# Sinkholes detection in the post-mining Olkusz-Bolesław Region (southern Poland) using a drone-based thermal camera

Marcin WÓDKA[1, *], Sylwester KAMIENIARZ[1], Jakub CURYŁO[1], Tomasz WOJCIECHOWSKI[1], Mariusz ZAJĄC[1] and Jarosław KOS[1]

[1] Polish Geological Institute – National Research Institute, Geohazards Center, Skrzatów 1, 31-560 Kraków, Poland; ORCID: 0000-0003-1591-3980 [M.W.], 0000-0002-8662-0491 [S.K.], 0000-0001-5858-0026 [T.W.], 0000-0002-8971--6237 [J.K.]

Wódka, M., Kamieniarz, S., Curyło, J., Wojciechowski, T., Zając, M., Kos, J., 2025. Sinkholes detection in the post-mining Olkusz-Bolesław Region (southern Poland) using a drone-based thermal camera. Geological Quarterly, **69**, 27; https://doi.org/10.7306/gq.1800

Sinkhole activity in the post-mining region of Olkusz and Bolesław (southern Poland) has intensified following recent hydrogeological changes. We introduce a novel approach using Unmanned Aerial Vehicle (UAV)-based thermal imaging to detect and predict sinkholes, focusing on shallow mining-induced voids. Two study areas were analysed: a test area with numerous known sinkholes and a predictive area with high sinkhole formation potential. Thermal orthomosaics, generated from drone flights conducted at sub-zero temperatures, revealed positive thermal anomalies associated with newly formed or reactivated sinkholes, attributed to heat flow from subsurface voids, and negative anomalies in older, stable depressions. This method successfully identified high-risk locations, though some anomalies were influenced by external factors (e.g., buildings, snow cover, stored objects). The results show that UAV-based thermal imaging is effective for making inventories of recent sinkholes and holds promise for predicting their occurrence, particularly in dynamic hydrogeological settings.

Key words: sinkholes detection, thermal camera, Unmanned Aerial Vehicle, geohazards.

## INTRODUCTION

Sinkholes in Poland have various origins. They are associated with both natural processes such as karst or suffosion, but they can also result from failures related to unexpected water outflows and soil erosion or be a consequence of underground mining activities. Although both natural sinkholes and those related to failures have often posed risks (e.g., Wojciechowski et al., 2024a, b), the most significant group appears to be those related to mining activities. One of the largest sinkhole disasters in Poland occurred in Wapno (Greater Poland Voivodeship) in 1977, where uncontrolled flooding of a salt mine led to the formation of massive sinkholes that destroyed 40 buildings and a section of a railway line. There were no casualties, but ~1400 people were evacuated (Małachowski, 2018; Kim et al., 2021). Mining-induced sinkholes have been and are still forming in regions such as Wałbrzych (Kozłowska-Woszczycka and Pactwa, 2024), Upper Silesia (Strozik et al., 2016; Strozik, 2018; Strzałkowski and Strzałkowska, 2023; Strzałkowski 2024), and Trzebinia (Kleta and Plewa, 2001; Frolik, 2006; Wódka et al., 2024). Recently, the Olkusz and Bolesław area has been characterized by an increasing sinkhole hazard (Kos et al., 2025), where the problem has intensified due to (sometimes rapid) changes in hydrogeological conditions following the closure of mines and cessation of their dewatering.

Predicting sinkholes is challenging due to the dynamic nature of the phenomena and frequent gaps in geological and mining documentation. A general review of sinkhole prediction methods was provided by Sahu and Lokhande (2015). In Poland, the Chudek-Olaszowski and Janusz-Jarosz method is commonly used (Chudek et al., 1988), which requires only determining the depth and height of the void and the thickness of the unconsolidated overburden above the void. Another approach involves identifying areas most susceptible to sinkhole formation based on similar geo-environmental factors as in regions where such phenomena have already occurred (Wódka et al., 2024). A comprehensive inventory of sinkholes is crucial for determining the factors conditioning their development in a given area (Papadopoulou-Vronitoti et al., 2013; Wódka et al., 2024). For mining-induced sinkholes, key factors include: exploitation depth up to 100 m b.g.l., exploitation with roof caving system, areas of overlapping exploited seams, fluctuations in groundwater levels, and the presence of old, filled sinkholes. Increased rainfall also plays a significant role in sinkhole development (e.g., Chudek et al., 1988; Xiao et al., 2018). In Poland, areas at risk of mining-induced sinkholes are typically delineated only by the boundaries of so-called “shallow exploitation” (Chudek et al., 1988), i.e., mining conducted up to 100 m b.g.l.

* Corresponding author, e-mail: mwod@pgi.gov.pl
Received: May 8, 2025; accepted: July 3, 2025; first published online: September 22, 2025

A significant challenge is that areas predisposed to discontinuous deformation are usually large, making it difficult to predict the exact location of a sinkhole. To address this, indirect methods (typically geophysical) and direct methods, such as drilling, are employed in the most threatened areas. A review of geophysical methods used to study discontinuous deformation was compiled by Fajklewicz et al. (2004) and Popiołek and Pilecki (2006). Commonly used methods for identifying weakened zones in the ground include gravimetry, ground-penetrating radar (GPR), seismics, and electrical resistivity tomography. The choice of geophysical method depends on the lithology of the overburden above underground voids and the depth of the groundwater table. Efforts to detect early sinkhole threats have also involved combining data from airborne laser scanning, satellite radar interferometry, and analysis of minor surface changes in sinkhole-prone areas (Intrieri et al., 2015; Walczak et al., 2025). Direct methods include drilling and probing to detect subsurface voids.

A novel method, previously unused in Poland, is thermal imaging using an unmanned aerial vehicle (UAV). Although temperature change measurements in areas with existing sinkholes have been conducted in isolated cases (e.g., Pilecki and Popiołek, 2010), they have not been applied at larger scale. Today, with the increasing availability of UAVs and remote thermal cameras, it is possible to monitor ground temperature changes over large areas at limited cost, which may aid in predicting specific locations at risk of sinkhole formation. The use of thermal cameras and UAVs for sinkhole detection is not widespread globally, though tests were conducted as early as 2016 to explore early sinkhole prediction possibilities (Lee et al., 2016). We describe the results of a pilot study to record and predict sinkholes using a drone-based thermal camera in the Olkusz and Bolesław area.

## STUDY AREA AND GEOLOGICAL SETTING

The study area is located in southern Poland, in the Małopolskie Voivodeship, Olkusz County, within the region of former Zn-Pb ore exploitation (Fig. 1). The test area (A; 0.14 km) is situated on the border of the Bolesław and Olkusz municipalities, ~1 km south of national road no. 94, between Dojazdowa Street and railway lines no. 62 and 65. It is a forested area with elevations ranging from 309 to 338 m a.s.l., with an average slope of 8°. Its western part includes a section of a sand quarry, where local terrain variations exceed 20 m and slope inclinations reach 20°. The predictive area (B; 0.17 km) is located in Bolesaw, south of Gówna Street (Fig. 1). Its southern part consists mainly of forests and wastelands covering old open-pit workings and dumps. A section of the city bypass runs through the southeastern part of the area. The northern part features buildings and infrastructure. The terrain spans elevations from 309 to 343 m a.s.l., with an average slope of 5°.

The geological structure of the study areas primarily comprises Middle and Upper Triassic formations and Quaternary deposits (Kurek and Preidl, 1992, 1993; Kurek et al., 1994, 1999). The Middle Triassic is represented mainly by bedded limestones, commonly marly, conglomeratic limestones, coarsely crystalline limestones with cherts, finely crystalline limestones, wavy and brecciated limestones with abundant fauna, and finely crystalline limestones. Due to metasomatic alteration, finely crystalline ore-bearing dolomites formed within these formations. These are highly compact but characterized by caverns, dense fracture networks, and the presence of clayey and calcitic dolomite breccias. Zinc and lead ores, with thicknesses reaching several metres, occur within these formations and have been mined since the 13th century (Siemiradzki, 1912). In the upper parts of the Middle Triassic, highly cavernous *Diplopora* dolomites are present.

Upper Triassic formations are preserved only in the western part of the area, within a WNW–ESE trending tectonic trough, and consist of grey siltstones with carbonate interbeds. The total thickness of Triassic formations in the study areas ranges from 52–101 m in the eastern part and 62–108 m in the western part (Kurek and Preidl, 1992; Kurek et al., 1999).

Quaternary deposits with greater thickness occur mainly in the eastern and central parts of the region (Fig. 2). These are predominantly sands and gravels from glaciofluvial accumulation and fine-grained aeolian sands preserved as dunes. Their total thickness locally reaches 40–50 m (Kurek and Preidl, 1992). In the western part, the Quaternary cover is significantly thinner (up to 14 m) or absent (Kurek et al., 1999; Fig. 2). On valley slopes, sands and clays containing Triassic rock fragments are found. In the northwestern part, on the highest elevations, loess covers are present. Anthropogenic soils in the form of embankments and dumps are widespread throughout the area.

In the Olkusz region, comprehensive sinkhole inventories, including of currently filled ones, were conducted between 2024 and 2025 (Kos et al., 2025). Based on archival data, historical aerial photographs, satellite imagery, digital terrain models, and primarily field surveys, 1,260 sinkholes were identified. In area A, there were 156 sinkholes, and in area B, 72 sinkholes.

## METHODOLOGY

### METHODOLOGICAL ASSUMPTIONS

Underground workings contain natural sources of heat inflow. For shallow workings – up to 100 m b.g.l., which are significant for sinkhole development in Poland – the geothermal gradient is less critical than in deeper workings. However, the temperature in now-abandoned, unventilated workings is likely >0°C. Additionally, the rising groundwater level, which has already filled many workings, contributes to maintaining a positive temperature. Cracks and loosenings in the ground, which precede sinkhole development, can create channels for heat flow from deeper layer of the rock mass. In winter, this heat flow should increase the temperature of the near-surface ground. In summer, the trend reverses, with areas of sinkhole initiation exhibiting lower temperatures due to intense surface heating. We assumed that thermal anomalies would be particularly visible when air temperatures are negative or close to 0°C. Methods of locating heat flow channels in winter have proven useful, for example, in locating cave openings or crevices in the Kraków-Częstochowa Upland, where the temperature of caves is approximately constant and ranges from ~6 to 8°C (Górny and Szelerewicz, 1986). In winter, in places where warmer air escapes over crevices leading to previously unknown caves, melting of the snow cover has been observed.

The Olkusz region is prone to sinkholes, particularly in areas of old, filled shafts or sinkholes, whose exact locations are

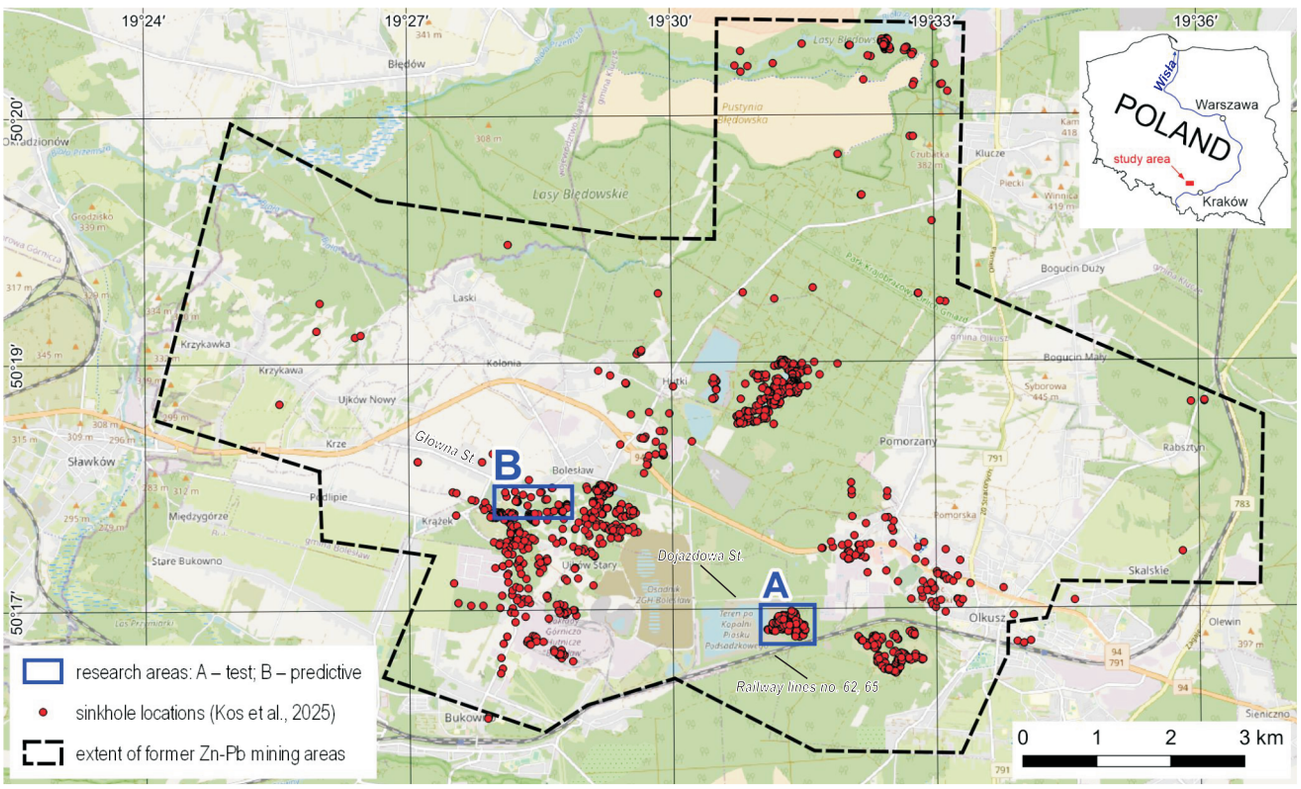


**Fig. 1. Location of the study area**

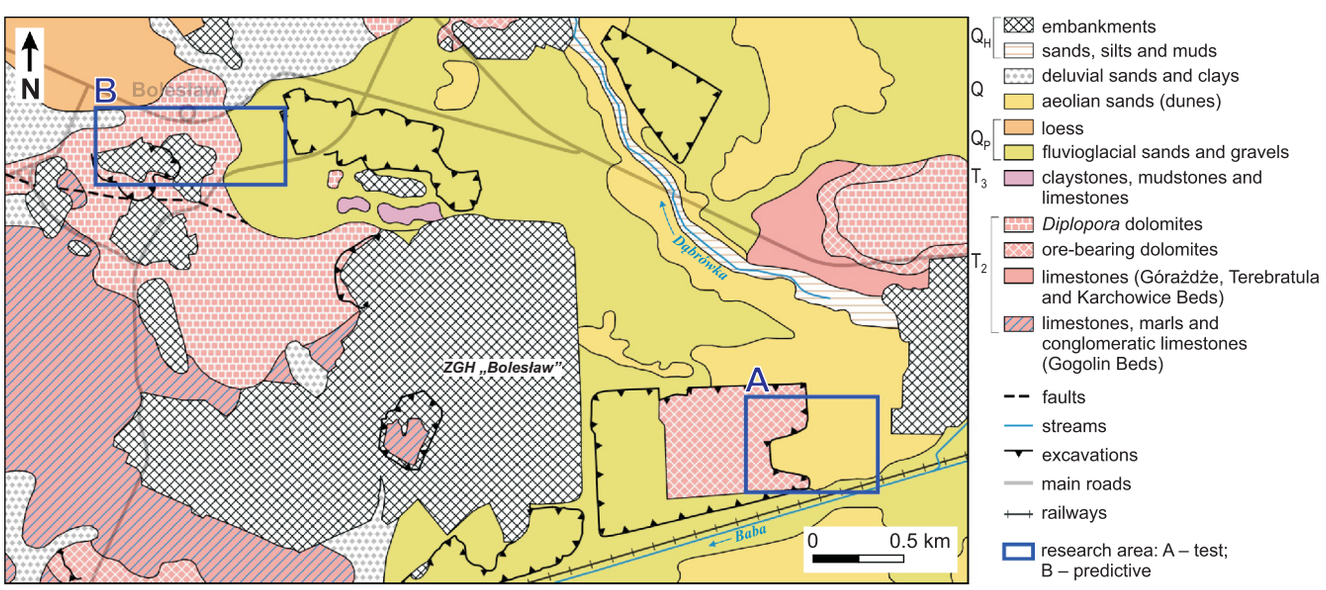


**Fig. 2. Simplified geological sketch**
**(based on Kurek and Preidl, 1992; Kurek et al., 1999; Bednarczyk, 2014; modified)**

difficult to determine (Kos et al., 2025). Unlike dolomites, which have low thermal conductivity, a shaft filled with backfill material or an old sinkhole filled with less consolidated material can act as a heat flow channel from deeper layers of rock mass, especially shortly before a sinkhole develops. In the case of shallow mining workings collapsing, a secondary void and fracture zone migrate upwards to the surface or to the boundary between solid rock and unconsolidated Quaternary overburden (Chudek et al., 1988). The development of cracks, fractures, and soil loosenings, often resulting from increased suffosion of unconsolidated Quaternary overburden, can serve as heat flow channels from underground voids, causing thermal anomalies at the surface.

To assess the potential of a Drone-Based Thermal Camera in sinkhole research, two study areas were selected. The drone flight over the first area (A) aimed to confirm methodological assumptions regarding thermal anomalies over existing sinkholes. The flight over the second area (B) was intended to test the method's ability to predict sinkhole occurrences.

### TEST AREA A

To test the methodological assumptions, an area with a large number of sinkholes, both old and those formed after 2020 (following mine flooding), was selected. Mining in this area was conducted with roof collapse, and in the central part of the area sinkholes were not reclaimed. The presence of many sinkholes of varying ages allowed for tracking potential thermal anomalies. The timing of sinkhole formation was determined using multi-temporal laser and satellite data from the Head Office of Geodesy and Cartography (GUGiK) and orthophotomaps created from UAV flights for this study.

### PREDICTIVE AREA B

To evaluate the potential of the drone-based thermal camera for assessment of early sinkhole predisposition, an area with high sinkhole formation dynamics but fewer sinkholes was chosen. Based on historical mining maps from the Polish State Mining Authority and historical aerial photographs, numerous now-abandoned shafts and old, filled sinkholes were identified (Kos et al., 2025). Due to its proximity to buildings and infrastructure, this area has a higher sinkhole risk.

### WEATHER CONDITIONS

Limited equipment availability allowed measurements to be conducted on only one day, selected as the last day with forecasted negative temperatures during the day and night. Subsequent days were expected to bring warmer temperatures 0°C. The first drone flight before sunrise was not feasible due to unexpectedly low temperatures <–10°C, which, according to the manufacturer's specifications, were unsafe for the thermal camera. Flights were conducted on February 21, between 7:40 AM and 11:40 AM. For the test area (A), one mission was flown at ~–7°C. For the predictive area (B), two missions were conducted: one at –8°C and another at ~–2°C. To minimize disturbances associated with thermal measurements after sunrise (Lee et al., 2016; Fiorucci et al., 2018; Loiotine et al., 2022), thermal imaging was performed in short time intervals over small areas to limit their impact on the resulting temperature distribution in the thermal image.

### DATA ACQUISITION AND PROCESSING

Measurement missions were conducted using a DJI Mavic 3 Thermal drone equipped with a VOx Microbolometer thermal camera and a wide-angle RGB camera with a 1/2" CMOS sensor. Due to the need to perform photogrammetric flights in the shortest possible time and the low resolution of thermal images (640 x 512 pixels), missions were conducted at a height of 70 m a.g.l. This altitude balanced flight time and the resulting thermal image resolution. Lower altitudes would provide higher resolution but pose challenges in mission execution (battery limitations) and data post-processing. Drone flights involved simultaneous recording of thermal images and digital photographs, the latter being essential for creating a digital orthophotomap covering the same measurement range (two layers over the same area with identical flight parameters).

The acquired digital data were processed in Agisoft Metashape Professional to produce a true-colour RGB orthomosaic and a thermal orthomosaic depicting changes of temperatures (warmer and cooler areas) which was sufficient for the purpose of analysis. Absolute temperature values were not obtained, probably due to insufficient thermal compensation of the camera's sensor under the prevailing weather conditions (during the mission, temperatures ranged from –2 to –8°C), thermal drift errors, using a single value of emissivity factor for the entire thermal image, and imprecise NUC (Non-Uniformity Correction) calibration before the start of the photoflight mission. Despite these limitations, the temperature changes in the thermal images recorded were reproduced correctly, but in this case, the numerical values of temperature changes are indicative and qualitative rather than quantitative. Determining real temperature values would require determining many reference points on different ground surfaces and measuring their temperatures at the time of flight.

Identifying sinkholes based on ground temperature differences required excluding errors related to the camera's measurement accuracy (rejection of single pixels indicating temperature differences) and areas with temperature variations due to other factors, such as local snow cover, vegetation shading (flights were conducted shortly after sunrise), shallow groundwater, buildings, and power lines. Verification involved analysing the orthophotomap created simultaneously with the thermal measurement and excluding these factors in areas with observed anomalies. Sinkhole registration was primarily based on the shape of the anomaly covering more pixels, which is typically oval or elliptical for sinkholes.

## RESULTS

### TEST AREA A

Processing data from the drone flight over the test area revealed numerous temperature anomalies (Fig. 3). Most anomalies clustered in areas with sinkholes, but some were related to varied sunlight exposure (presence of shade), presence or absence of snow cover, and shallow groundwater (Fig. 4). Due to the absence of power lines in the test area and the homogeneity of the soils (predominantly sands), other causes of anomalies visible in the thermal orthomosaic were ruled out.

In the northern part of the area, a distinct positive anomaly with a circular shape was recorded, coinciding with a sinkhole formed between 2023 and 2024 and reactivated (widened and deepened) in 2025, shortly before the thermal measurements. One factor contributing to the elevated temperature in this sinkhole is the presence of shallow groundwater. According to the orthophotomap created during the thermal measurements, the sinkhole was dry at the time of recording. The proximity of groundwater to the surface was confirmed by a rectangular anomaly located directly north of the recently reactivated sinkhole (Fig. 4), corresponding to a man-made excavation, an old sand quarry, which was dry at the time of the flight but is now partially flooded. Less distinct positive anomalies were recorded for sinkholes reactivated between 2023 and 2024, with warmer ground observed only in the marginal parts of individual sinkholes.

The largest negative anomalies, with clearly elliptical shapes, were typically associated with old sinkholes formed before 2023, now forming depressions that maintain low temperatures


**Fig. 3. Thermal orthomosaic and Digital Terrain Model for the test area A**

(Fig. 3). These anomalies result from significant shading and prolonged snow cover duration.

The results corroborated the methodological assumptions, dividing sinkholes into two types: “older” ones formed before 2023, lacking heat flow channels, and “new” ones formed or re-activated after 2023, from which heat escapes to varying degrees. Older forms exhibited negative anomalies, while new sinkholes, including those expanding in recent years, showed positive anomalies.

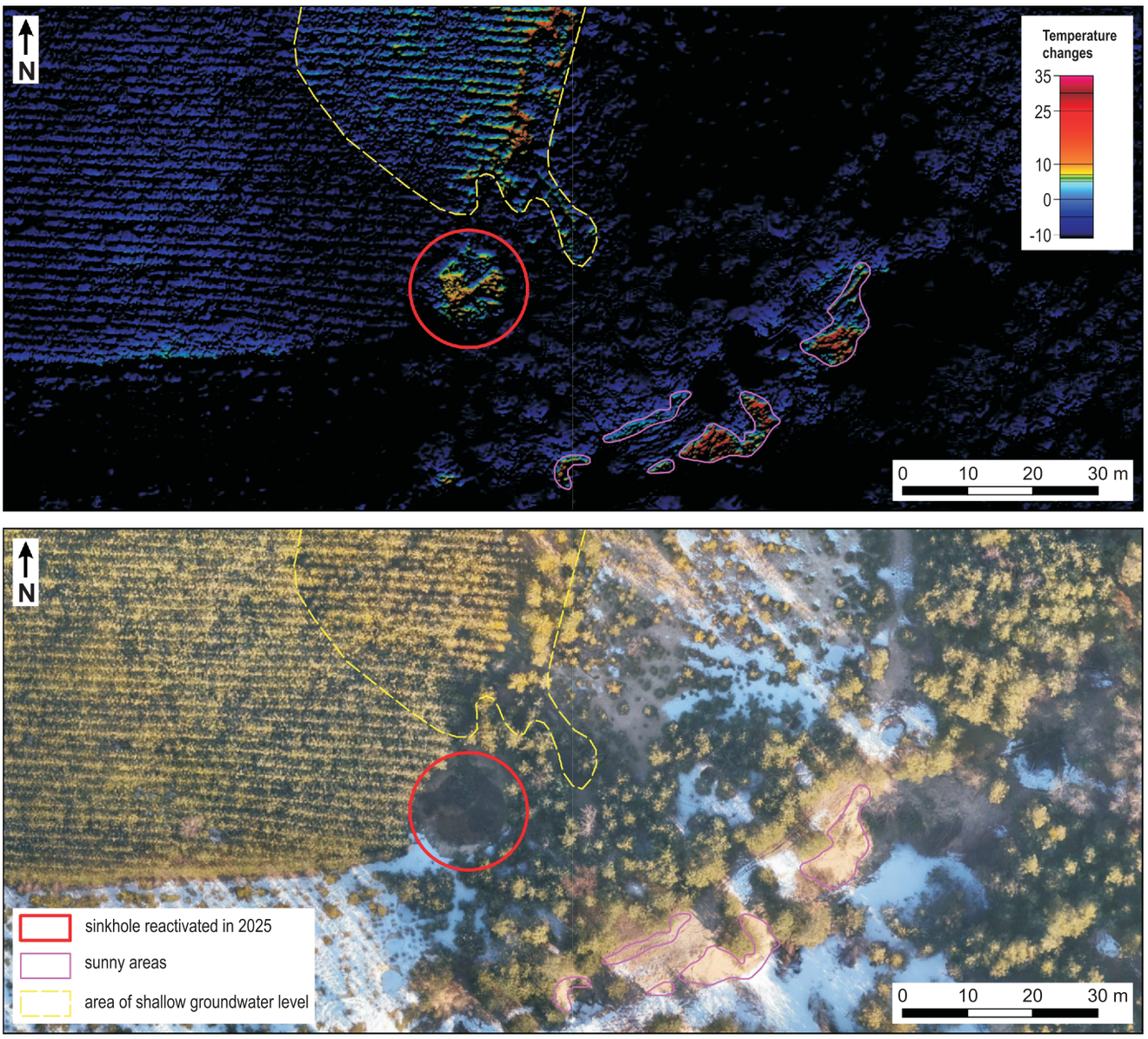


**Fig. 4. Thermal orthomosaic and orthophotomap for the northen part of the test area A**

PREDICTIVE AREA B

The thermal imaging of the predictive area is less varied but includes errors due to local snow cover, shadows (flights conducted at sunrise), buildings, photovoltaic panels, and stored items near buildings. Two positive anomalies with distinctly oval to circular shapes in the northwestern part of the area are noteworthy (Fig. 5A).

The first anomaly is located near the road leading to the cemetery and close to a supermarket parking lot. Despite its proximity to infrastructure, the area is unused due to a steep, artificially formed slope (~28°). Analysis of underground utility lines showed no direct connection to the anomaly. The anomaly has values similar to the "new" sinkhole in the northern part of test area A. Comparing the thermal orthomosaic with the orthophotomap ruled out the influence of shading from the supermarket, located ~23 m east of the anomaly. The anomaly's distinctly oval shape (Fig. 5B) suggests a potential sinkhole in the initiation stage with heat flow from below the surface. Historical mining maps do not indicate shallow workings in this location, but nearby galleries are marked, though their exact location is uncertain.

The second circular anomaly, with high positive values, is located near a service building on its southern side, occupying a small area with a radius of <1 m (Fig. 5C). Analysis ruled out the influence of shading or sunlight. The orthophotomap indicated the presence of multiple stored items near the building. Historical mining maps suggest an old, now-filled shaft in this location. Despite the limited accuracy of old maps, this site was identified as having increased risk due to its proximity to the service building.

Results from a subsequent drone flight conducted around 11 AM were unusable, with the thermal orthomosaic showing large, heterogeneously distributed changes of temperature that were difficult to interpret.

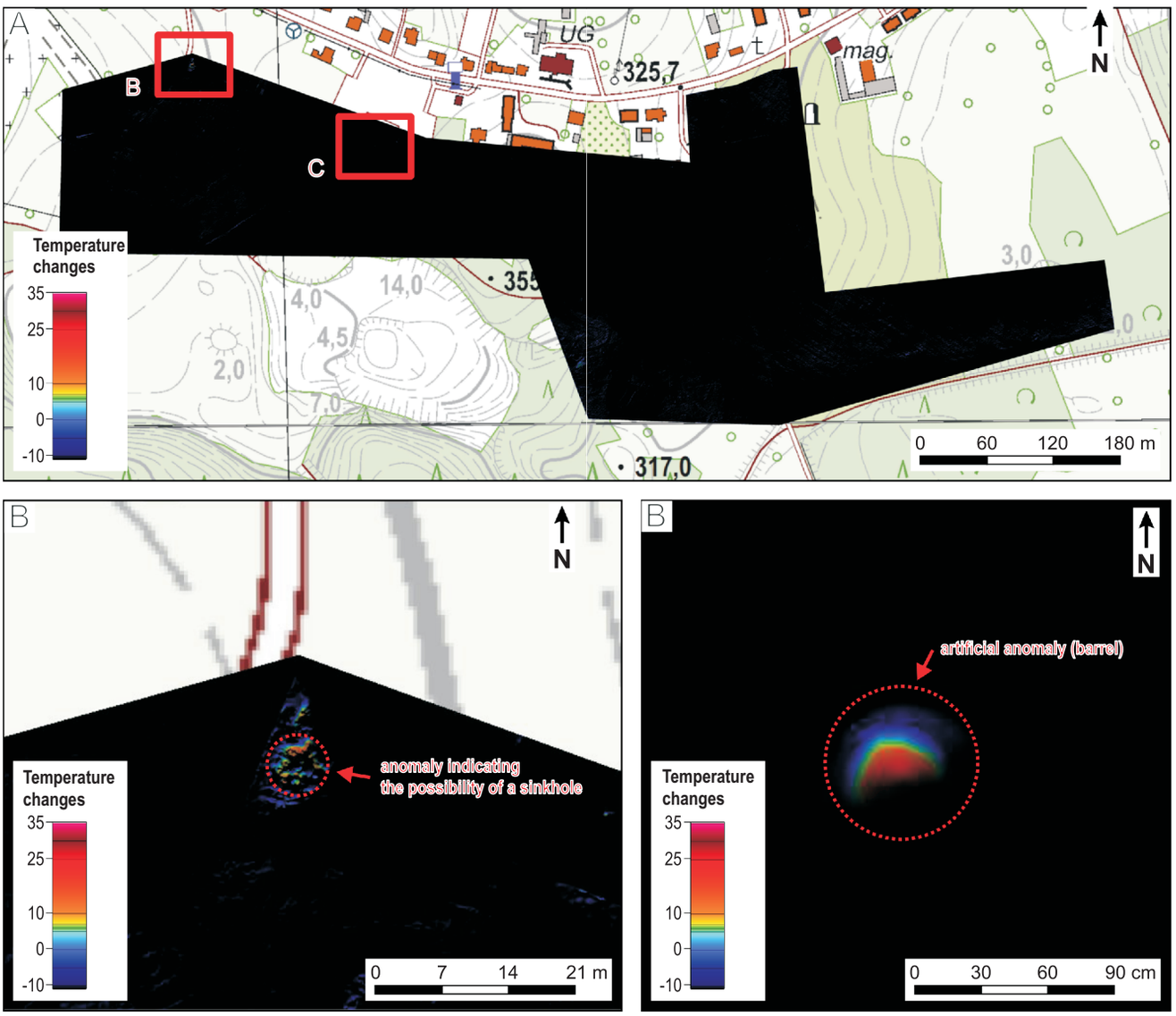


**Fig. 5. Thermal orthomosaic for the predictive area B (A) and zoom to two areas with positive anomalies (B, C)**

A week later, a field inspection was conducted to verify and assess the risk at the locations identified. At the first site, no sinkhole was found, but the presence of geotextile along the entire length of the artificial slope could have disturbed the measurement. However, due to the clearly circular shape of the anomaly at this place, leading to a decision to periodically monitor the area for potential terrain depressions. The second site was determined to be an error due to a barrel filled with waste, meaning the measurement recorded heat from the substance in the barrel rather than the ground.

## DISCUSSION

Tests conducted in the post-mining areas of Olkusz and Bolesław confirm the possibility of using a thermal camera mounted on a drone to inventory sinkholes, especially newly created. The confirmation of methodological assumptions in the test area suggests that thermal imaging can also support sinkhole prediction, although, as of the writing of this article, no sinkhole has formed at the location of the distinct positive anomaly identified in the predictive area. The use of a thermal camera can serve as an indirect method to refine the most hazardous locations within larger areas previously identified. These larger areas can be determined based on the extent of shallow exploitation (Chudek et al., 1988; Strzałkowski et al., 2021), the Chudek-Olaszowski and Janusz-Jarosz methods (Chudek et al., 1988), or by identifying geo-environmental similarities based on comprehensive sinkhole inventories (Wódka et al., 2024).

In the Olkusz region, where many sinkholes are associated with the reactivation of filled sinkholes or shafts, and information on their exact locations is subject to 10–20 m errors (Kos et al., 2025), the use of a thermal camera on a drone can be highly useful. Thermal anomalies related to an abandoned shaft in the Olkusz area were confirmed by Pilecki and Popiołek (2010), but observations were limited to a single case. The use of UAV enables the analysis of thermal changes over large areas, particularly when approximate locations of historical shafts are known,

allowing for risk assessment related to potential sinkhole reactivation and refining their locations. Therefore, future plans within the Polish geological survey include using a thermal camera with improved parameters to obtain higher-resolution thermal orthomosaics.

Initial attempts to detect artificially constructed sinkholes using a thermal camera on a drone were described by Lee et al. (2016). The measurements in the Olkusz area were the first documented use of a thermal camera on a drone in Poland, confirming the capabilities of these tools for both detection and prediction of sinkholes. Lee et al. (2016) noted that detecting voids filled with water is significantly easier. Our research confirmed this, with the most pronounced anomaly in the test area occurring in a dry sinkhole, but with groundwater very close to the surface, as indicated by anomalies in a nearby excavation. Water likely filled the voids below the surface, washing out natural backfill material and causing instability that led to sinkhole formation. The distinct anomaly in the then-dry excavation suggests potential of the method for floodplains predicting related to rising water levels and alerting for previously unpredicted locations.

Unlike Lee et al. (2016), our test was conducted in winter conditions, focusing on positive anomalies. Regional climatic conditions, with temperatures dropping below zero in winter, enable such tests. This period also coincided with increased sinkhole activity due to rising groundwater levels following the cessation of mine dewatering. Our results indicate that thermal imaging is effective at negative temperatures, and winter measurements may be more appropriate due to convection phenomena. Future plans include conducting drone flights at slightly higher temperatures (close to 0°C). The lack of more positive anomalies may be due to partial ground freezing, which at night temperatures below 10°C could affect loosenings and cracks forming heat flow channels.

Experience from initial tests suggests that the method performs best on cloudy days or after dusk. The second flight over the predictive area at 11 AM did not yield expected results, with thermal imaging showing a mosaic of colors that was difficult to interpret. The negative impact of sunlight was noted by Lee et al. (2016), Fiorucci et al. (2018), and Chang et al. (2025). Conducting thermal imaging with a drone after sunrise can cause disturbances in the resulting temperature distribution due to rapid surface heating by sunlight, varying heating rates of materials (e.g., asphalt, water, grass, soil), low sun angles increasing shadow lengths (mosaic heating effect), and challenges with thermal camera calibration, which requires stable temperature conditions. These factors can lead to temperature distribution disturbances in thermal images, complicating interpretation. The method is likely more effective in open areas where vegetation, trees, and buildings do not interfere with measurements.

Results from the test area indicate that the method is most effective in areas with high sinkhole dynamics, predicting locations that may collapse within days, weeks, or months. Studies on sinkhole dynamics in the Olkusz region identified 37 sinkholes in the test area over the past five years (Kos et al., 2025). As long as groundwater levels remain unstable, the dynamics of these phenomena will likely remain high. However, the thermal camera did not identify clear anomalies that would indicate the development of new sinkholes in the test area, where mining was conducted with roof caving. Furthermore, sinkholes formed ~1.5 years before the test showed no positive anomalies. Older sinkholes exhibited negative anomalies due to depressions and associated shading, unrelated to subsurface conditions. These anomalies are not related to heat transfer channels from underground voids, thus older sinkholes are likely not at risk of further expansion.

The test area results also suggest that the thermal camera can be used for terrain monitoring, ideally after a comprehensive sinkhole inventory. The method is partially effective for inventorying old sinkholes (cold anomalies) but can be used to detect new sinkholes with positive anomalies. This has economic implications, as monitoring with laser scanners is significantly more expensive due to the need for larger drones and heavier equipment.

## CONCLUSIONS

A thermal camera mounted on a drone can provide significant support for monitoring areas at risk of sinkholes.

At negative air temperatures, newly formed sinkholes are characterized by positive thermal anomalies. These anomalies can also be used to predict potential sinkhole locations.

The ground temperature measurement method is most effective in areas with high sinkhole dynamics, particularly where groundwater levels are approaching the surface. Effectiveness of the camera depends on the age of the form; young sinkholes are the easiest to detect.

The described method can also be used to predict floodplain related to rising water levels and to alert for previously unpredicted locations.

Analysis of thermal imaging results should be conducted concurrently with analysis of simultaneous ortophotomaps, utility maps, and mining and geological materials to avoid errors in interpretion.

Reliable results require measurements under appropriate conditions. The method is most effective at negative temperatures, on cloudy days or at night, in areas without snow cover and with limited vegetation.

## REFERENCES

**Bednarczyk, S., 2014.** The issue of using accompanying mineral on the basis of “Pustynia Błędowska – blok IV” deposit exploitation (in Polish with English summary). Przegląd Górniczy, **70:** 147–154.

**Chang, B., Hwang, B., Lim, W., Kim, H., Kang, W., Park, Y.-S., Ko, D.W., 2025.** Enhancing wildlife detection using thermal imaging drones: designing the flight path. Drones, **9**, 52; https://doi.org/10.3390/drones9010052

**Chudek, M., Janusz, W., Zych, J., 1988.** Studium dotyczące rozpoznania tworzenia się i prognozowania deformacji nieciągłych pod wpływem podziemnej eksploatacji złóż (in Polish). Zeszyty Naukowe Politechniki Śląskiej, seria Górnictwo, **141**.

**Fajklewicz, Z., Piwowarski, W., Radomiński, E., Stewarski, E., Tajduś, A., 2004.** Rock-mass deformation changes research for restoration of building ground value (in Polish). Agencja Wydawniczo-Poligraficzna Art-Tekst, Kraków.

**Fiorucci, M., Marmoni, G.M., Martino, S., Mazzanti, P., 2018.** Thermal response of jointed rock masses inferred from infrared thermographic surveying (Acuto test-site, Italy). Sensors, **18**, 2221; https://doi.org/10.3390/s18072221

**Frolik, A., 2006.** Up-dating of the forecast for flooding of "Siersza" mine (in Polish with English summary). Wiadomości Górnicze, **57**: 616–624.

**Górny, A., Szelerewicz, M. (eds.), 1986.** Jaskinie Wyżyny Krakowsko-Wieluńskiej (in Polish). Wydaw. PTTK Kraj, Warszawa.

**Intrieri, E., Gigli, G., Nocentini, M., Lombardi, L., Mugnai, F., Fidolini, F., Casagli, N., 2015.** Sinkhole monitoring and early warning: an experimental and successful GB-InSAR application. Geomorphology, **241**: 304–314; https://doi.org/10.1016/j.geomorph.2015.04.018

**Kim, T.T.H., Tran, H.H., Bui, K.L., Lipecki, T., 2021.** Mining-induced land subsidence detected by Sentinel-1 SAR images: An example from the historical Tadeusz Kościuszko Salt Mine at Wapno, Greater Poland Voivodeship, Poland. Inżynieria Mineralna, **2**: 4152; https://doi.org/10.29227/IM-2021-02-04

**Kleta, H., Plewa, F., 2001.** Risk for ground surface after long termmining exploration on the example of "Siersza" mine (in Polish with English summary). Zeszyty Naukowe. Górnictwo, **250**: 141–151.

**Kos, J., Wojciechowski, T., Zając, M., Kamieniarz, S., Przyłucka, M., Perski, Z., Karwacki, K., Wódka, M., Warmuz, M., Jureczka, J., Nadłonek, W., Rycio, E., Nescieruk, P., Sikora, R., Curyło, J., Budziński, D., Walicka, A., Balicki, L., Rolka, M., Krieger, W., Ługiewicz-Mołas, I., Hadro, J., Suszka, G., Strzemińska, K., Górka, K., Rudnicki, A., Ściurka, A., 2025.** Raport z prac analitycznych o deformacjach terenu dla rejonu oddziaływania eksploatacji rud cynku i ołowiu w rejonie olkuskim (in Polish). Państwowy Instytut Geologiczny – Państwowy Instytut Badawczy, Warszawa. https://www.pgi.gov.pl/rejon-olkuski-2

**Kozłowska-Woszczycka, A., Pactwa, A., 2024.** Diagnosis of the Walbrzych post-mining area: pilot study using social participation. The Extractive Industries and Society, **17**, 101401; https://doi.org/10.1016/j.exis.2023.101401

**Kurek, S., Preidl, M., 1992.** Szczegółowa mapa geologiczna Polski w skali 1:50 000, arkusz Olkusz (in Polish). Państwowy Instytut Geologiczny, Warszawa.

**Kurek, S., Preidl, M., 1993.** Objaśnienia do Szczegółowej mapy geologicznej Polski w skali 1:50 000, arkusz Olkusz (in Polish). Państwowy Instytut Geologiczny, Warszawa.

**Kurek, S., Paszkowski, M., Preidl, M., 1994.** Objaśnienia do Szczegółowej mapy geologicznej Polski w skali 1:50 000, arkusz Jaworzno (in Polish). Państwowy Instytut Geologiczny, Warszawa.

**Kurek, S., Paszkowski, M., Preidl, M., 1999.** Szczegółowa mapa geologiczna Polski w skali 1:50 000, arkusz Jaworzno (in Polish). Państwowy Instytut Geologiczny, Warszawa.

**Lee, E.J., Shin, S.Y., Ko, B.C., Chang, C., 2016.** Early sinkhole detection using a drone-based thermal camera and image processing. Infrared Physics & Technology, **78**: 223–232; https://doi.org/10.1016/j.infrared.2016.08.009

**Loiotine, L., Andriani, G.F., Derron, M,-H., Parise, M., Jaboyedoff, M., 2022.** Evaluation of InfraRed thermography supported by UAV and field surveys for rock mass characterization in complex settings. Geosciences, **12**, 116; https://doi.org/10.3390/geosciences12030116

**Małachowski, K., 2018.** The biggest surface mining disaster in Poland and its economic results. European Journal of Service Management, **9**: 247–255; https://doi.org/10.18276/ejsm.2018.28/2-31

**Papadopoulou-Vrynioti, K., Bathrellos, G.D., Skilodimou, H.D., Kaviris, G., Makropoulos, K., 2013.** Karst collapse susceptibility mapping considering peak ground acceleration in a rapidly growing urban area**.** Engineering Geology, **158**: 77–88; https://doi.org/10.1016/j.enggeo.2013.02.009

**Pilecki, Z., Popiołek, E., 2010.** Geodezyjne i geofizyczne rozpoznanie zagrożenia zapadliskowego (in Polish). Bezpieczeństwo Pracy i Ochrona Środowiska w Górnictwie, **6**: 34–39.

**Popiołek, E., Pilecki, Z., 2006.** Comparison of geophysical and geodetic methods used for discontinuous deformation recognition on post-mining areas of zinc and lead mines. In: Altbergbau-Kolloquium (eds. W. Frenz, A. Preuße, G. Meier, A. Sroka, K.-H. Löbel, H. Klapperich, D. Tondera, W. Busch, K. Maas and P.N. Martens): 6. Essen VGE, Verl. Glückauf, Aachen/Alsdorf.

**Sahu, P., Lokhande, R.D., 2015.** An investigation of sinkhole subsidence and its preventive measures in underground coal mining. Procedia Earth and Planetary Science, **11**: 63–75; https://doi.org/10.1016/j.proeps.2015.06.009

**Siemiradzki, J., 1912.** Płody kopalne Polski (in Polish). Lwów.

**Strozik, G., 2018.** The use of fly ash for filling the shallow underground ore mine works on the example of the mine reclamation area in Piekary Śląskie. Gospodarka Surowcami Mineralnymi, **34**: 139–154; https://doi.org/10.24425/118637

**Strozik, G., Jendruś, R., Manowska, A., Popczyk, M., 2016.** Mine subsidence as a post-mining effect in the Upper Silesia Coal Basin. Polish Journal of Environmental Studies, **25**: 777–785; https://doi.org/10.15244/pjoes/61117

**Strzałkowski, P., 2024.** Influence of the Depth of Shallow Workings on the Probability of Sinkhole Formation and Determination of the Contribution of Mines to the Resulting Risk. Pure and Applied Geophysics, **181**: 3121–3131; https://doi.org/10.1007/s00024-024-03583-0

**Strzałkowski, P., Strzałkowska, E., 2023.** An assessment of the impact of the degree of the filling of shallow voids on the possibility of sinkhole formation on the surface. Gospodarka Surowcami Mineralnymi, **39**: 173–191; https://doi.org/10.24425/gsm.2023.144627

**Strzałkowski, P., Ścigała R., Szafulera, K., Kołodziej, K., 2021.** Surface deformations resulting from abandoned mining excavations. Energies, **14**, 2495; https://doi.org/10.3390/en14092495

**Walczak, S., Witkowski, W.T., Stoch, T., Guzy, A., 2025.** Detecting sinkholes and land surface movement in post-mining regions using multi-source remote sensing data. Remote Sensing Applications: Society and Environment, **38**, 101560; https://doi.org/10.1016/j.rsase.2025.101560

**Wojciechowski, T., Laskowicz, I., Kos, J., Marciniec, P., Uścinowicz, G., Karkowska, K., Przyłucka, M., Wódka, M., Kamieniarz, S., 2024a.** Geohazards in Poland in 2022 (in Polish with English summary). Przegląd Geologiczny, **72**: 439–450; https://doi.org/10.7306/2024.25

**Wojciechowski, T., Wódka, M., Kamieniarz S., Kos, J., Karkowska, K., Laskowicz, I., Marciniec, P., Warmuz, B., Uścinowicz, G., Przyłucka, M., 2024b.** Geohazards in Poland in 2023 (in Polish with English summary). Przegląd Geologiczny, **72**: 671–684; https://doi.org/10.7306/2024.51

**Wódka, M., Kamieniarz, S., Wojciechowski, T., Przyłucka, M., Perski, Z., Sikora, R., Karwacki, K., Jureczka, J., Nadłonek, W., Krieger, W., Zając, M., 2024.** Post-mining deformations in the area affected by the former "Siersza" hard coal mine in Trzebinia (southern Poland). Geological Quarterly, **68**, 3; https://doi.org/10.7306/GQ.1726

**Xiao, H., Li, H., Tang, Y., 2018.** Assessing the effects of rainfall, groundwater downward leakage, and groundwater head differences on the development of cover-collapse and cover-suffosion sinkholes in central Florida. Science of the Total Environment, **644**: 274–286; https://doi.org/10.1016/j.scitotenv.2018.06.273